Dynamical localization transition in the non-Hermitian $\mathbb{Z}_2$ gauge theory

Jun-Qing Cheng,[1,2] Shuai Yin,[1,*] and Dao-Xin Yao[1,†]

[1]*State Key Laboratory of Optoelectronic Materials and Technologies, Guangdong Provincial Key Laboratory of Magnetoelectric Physics and Devices, School of Physics, Sun Yat-Sen University, Guangzhou 510275, China*

[2]*School of Physical Sciences, Great Bay University, Dongguan 523000, China*

(Dated: July 14, 2023)

I. QUENCH DYNAMICS FROM THE DOMAIN WALL INITIAL STATES

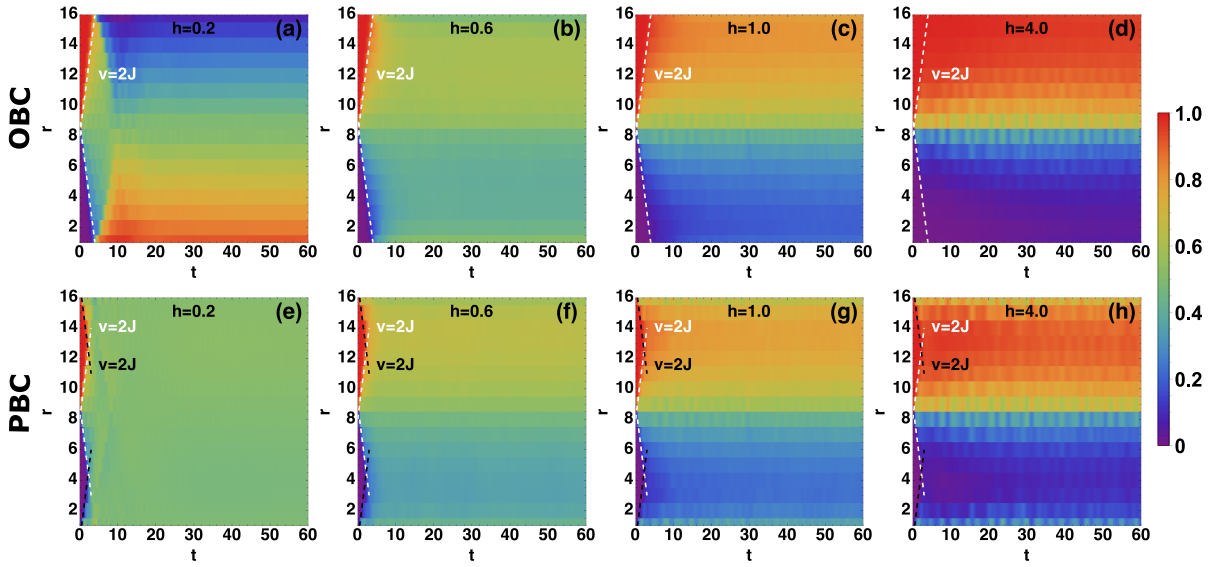

Supplementary Figure 1. **Dynamics of fermion density.** Dynamics of fermion density $\langle n_i(t)\rangle$ for the system with $L = 16$ under OBC and PBC at different h. The initial state of fermionic subsystem is domain wall state and the non-Hermiticity is chosen as $g = 0.2$. The white and black dashed lines represent the propagating signal, half of Lieb-Robinson velocity $v = v_{\mathrm{LR}}/2 = 2J$.

In this section, we consider the quench dynamics from the domain wall (DW) initial state $|0,\ldots,0,1,\ldots,1\rangle$. In Supplementary Figure 1, the dynamics of fermion density $\langle n(t)\rangle$ for the system with $L = 16$ under OBC and PBC are displayed. For the OBC case at $h = 0.2$, the non-Hermitian skin effect drives the fermions to propagate to the one side, meanwhile the holes transport to in opposite direction. Both the fermions and holes travel at the maximal fermion group velocity $2J$, also the one half of Lieb-Robinson velocity $v = v_{\mathrm{LR}}/2 = 2J$ [1, 2]. The weak effective disorder $h = 0.2$ is not strong to preserve the memory of initial DW state, and a approximate reverse DW state is presents due to the Pauli exclusion principle. As h is increased, the localization behaviour becomes more obvious and the memories of initial state are preserved. At the boundary of domain wall, large h also induces the distinct oscillation in the fermion density and leads the fermions or holes across the domain wall. For the PBC case, the non-Hermitian skin effect is disappear. There are two arches at the early time evolution since the two domain walls of initial state. The propagating velocities are still the maximal fermion group velocity $2J$. For the weak disorder, the fermions propagate throughout the system with extended states. The localization behaviour becomes more and more clearly as the h is increased. For strong disorder $h = 4.0$, some fermions and holes also pass through the two domain walls because of the oscillations.

* yinsh6@mail.sysu.edu.cn
† yaodaox@mail.sysu.edu.cn

II. ENTANGLEMENT DYNAMICS OF FERMIONS

The dynamics of entanglement entropy for an isolated system is a well-defined signature for differentiating between thermalization and localization. Here we focus on the evolution of the half-chain entanglement entropy for the effective system initialized in the CDW state. In supplementary Figure 2(a), except the Hermitian case $g = 0$, others $g \geq 0.2$ are in the delocalized phase. For $g = 0$, the entanglement entropy grows logarithmically after quench and eventually saturates to value. The main reason is that the wave functions initially spreads symmetrically in the two directions along the system, the entanglement entropy propagates throughout the whole system. After introducing the non-Hermiticity, the entanglement entropy initially still increases logarithmically, but the steady values decrease with the increase of g. The non-Hermitian skin effect leads to the antisymmetry spreading of fermionic wave functions and suppress the spreading process, which contributes to the nonequilibrium steady state with low entanglement entropy. Supplementary Figure 2(b) shows the effect of disorder strength on the dynamics of fermions in the localized phase, it can be observed that the entanglement entropy also increases logarithmically at the initial period, and the strong disorder also reduces the entanglement entropy of nonequilibrium steady state in the localized phase because of that the wave functions are localized and the entanglement propagations are suppressed. In the delocalized and localized phases, the entanglement entropies are both suppressed, but for different reason, the first is due to the non-Hermitian skin effect, the second is the consequence of strong effective disorder form the $\mathbb{Z}_2$ gauge field.

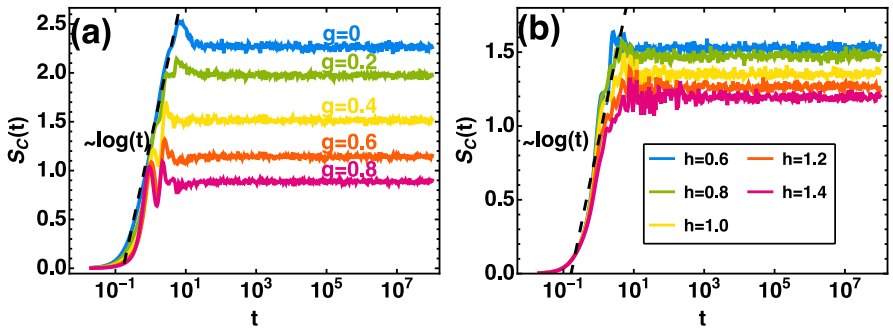

Supplementary Figure 2. **Dynamics of entanglement entropy.** Dynamics of entanglement entropy of fermion for the OBC with $L = 10$ (a) at different hopping strength g for $h = 0.5$ and (b) at different effective disorder strength h for $g = 0.4$. The initial state of fermionic subsystem is CDW state. The dashed lines correspond to the logarithmic growth behaviours.

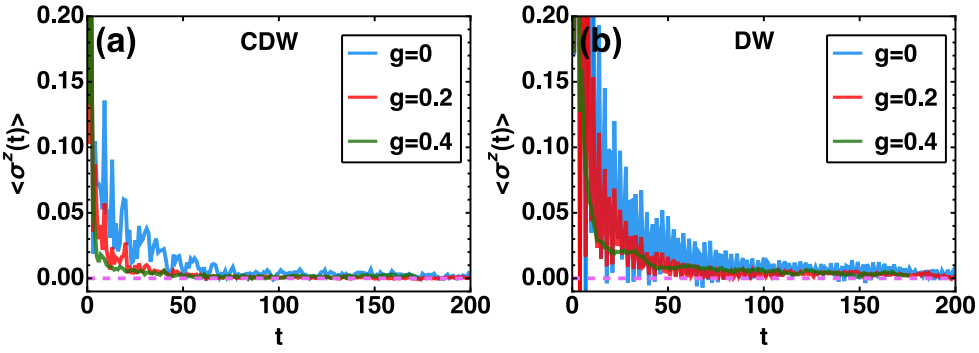

Supplementary Figure 3. **Dynamics of spin.** The time evolution of spin average $\langle\hat{\sigma}^z(t)\rangle$ for different g after a quench from the (a) CDW state, (b) DW state. All dynamics are measured under the same condition $L = 16$ and $h = 1$.

III. SPIN SUBSYSTEM

Above results mainly consider the dynamics of fermion subsystem, now let us turn to the spin subsystem. The spin correlators can be written as fermionic ones according to the evolution governed by the effective Hamiltonian (see Eq.(2) in the main text). For a polarized initial spin state, the disorder averaged over all charge configurations should be considered. An expectation value

of $\hat{\sigma}^z$ spin component on the bond at time t after quench is given by

$$\left\langle \hat{\sigma}^z_{j,j+1}(t) \right\rangle = \langle 0| e^{i\hat{H}t} \hat{\tau}^x_j \hat{\tau}^x_{j+1} e^{-i\hat{H}t} |0\rangle = \frac{1}{2^{L-1}} \sum_{\{q_i\}=\pm 1} \langle \Psi| e^{i\hat{H}(q)t} e^{-i\hat{H}(\overline{q}_{j,j+1})t} |\Psi\rangle \tag{1}$$

where $\overline{q}_{j,j+1}$ means the signs of the charges at j and $j+1$ opposite to the original ones. In supplementary Figure 3, the dynamics of spin average is displayed for the CDW and DW initial states. For the Hermitian case, the magnetizations both decay to zero with an asymptotic power laws. The spin subsystem reach its nonequilibrium states for a short time evolution along with the fluctuation, especially for the DW initial state, the fluctuation is more obvious. By comparison, the non-Hermiticity effectively suppress the fluctuation and result in the faster decay progresses no matter for the CDW or DW initial states. Although the non-Hermiticity originates from the fermion subsystem, we can still observe its effect on the dynamics of spin subsystem.

IV. TRANSFER MATRIX

In this section, we will introduce how to calculate the localization length by transfer matrix method[3–5]. This numerical method allows us to compute the Lyapunov exponents for eigenstates in the thermodynamic limit. The localization length is directly related to the Lyapunov exponents and quantify the characteristic length for the decay of localized wavefunctions. We consider the one-dimensional Hamiltonian with onsite binary disorder described by

$$\hat{H}_{\{q_i\}} = -J \sum_i (e^g \hat{C}^\dagger_i \hat{C}_{i+1} + e^{-g} \hat{C}^\dagger_{i+1} \hat{C}_i) + 2h \sum_i q_i \hat{C}^\dagger_i \hat{C}_i, \tag{2}$$

where we have omitted an overall energy shift $h \sum_i q_i$ which does not affect the localization length since there are no matrix elements between different charge sectors. An arbitrary single-particle state is given by

$$|\Psi\rangle = \sum_{n=0}^{N} \Psi_n \hat{C}^\dagger |\Omega\rangle, \tag{3}$$

where $|\Omega\rangle$ is the fermionic vacuum state and Ψ_n is the particle wave function, the probability amplitude to find the particle at site n. The single-particle Schrödinger equation $H|\Psi\rangle = E|\Psi\rangle$thus reduces to the recursion relation

$$Je^{-g}\Psi_{n+1} + +2hq_n\Psi_n + Je^{g}\Psi_{n-1} = E\Psi_n. \tag{4}$$

By introducing a transfer matrix, this Schrödinger equation can be written in a compact form by

$$\begin{pmatrix} \Psi_{n+1} \\ \Psi_n \end{pmatrix} = M_n \begin{pmatrix} \Psi_n \\ \Psi_{n-1} \end{pmatrix}, \tag{5}$$

where the transfer matrix is given by

$$M_n = \begin{pmatrix} J^{-1}(2hq_n - E)\, e^g & -e^{2g} \\ 1 & 0 \end{pmatrix}. \tag{6}$$

According to the Oseledec's theorem, the exponent of Lyapunov exponent γ_n are the eigenvalues of a limiting matrix

$$\Gamma = \lim_{L\to\infty} \left(Q_L Q_L^\dagger \right)^{1/2L}, \tag{7}$$

where $Q_L = \prod_{n=1}^{L} M_n$. The smallest Lyapunov exponent describes the slowest growth of the wave function, and also corresponds to the inverse of the localization length λ. In summary, the spectrum of the effective Hamiltonian in the localized phase is a discrete spectrum of exponentially localized wave functions, whose characteristic localization length is given by the inverse of the Lyapunov exponent of the transfer matrix product.

V. NON-HERMITIAN QUANTUM DISENTANGLED LIQUID

In the main text, we divide the system into three parts to make sure the two subsystems have same sizes for calculating the quantum mutual information. The area law scaling of fermions and volume law scaling of spins successfully reveal the exist of non-Hermitian quantum disentangled liquid in the localized and delocalized phases. In order to exclude the effect of partitioning method on the non-Hermitian quantum disentangled liquid, we also provides the results where the sizes of subsystem are unequal $A \neq B$, see supplementary Figure 4(a). Although the subsystems A and B have the same numbers of fermion sites comparing

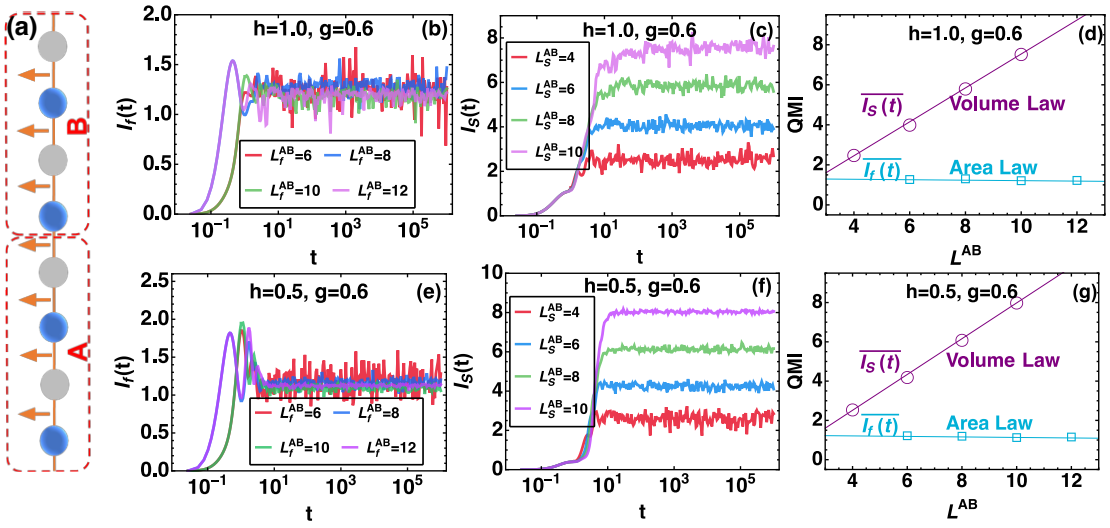

Supplementary Figure 4. **Features of non-Hermitian quantum disentangled liquid.** (a) The partitioning methods of the whole system. Dynamics of quantum mutual information for the fermion and spin subsystems with different sizes at the localized phase (b)(c)(d) $h = 1.0, g = 0.6$ and delocalized phase (e)(f)(g) $h = 0.5, g = 0.6$. The initial state is charge density wave state for fermion and the z-polarized state for spins. Saturation values $\overline{I_f(t)}$ and $\overline{I_S(t)}$ are averaged from $t = 10^3$ to $t = 10^6$ for different systems sizes. Here the OBC is considered.

of the case where $A = B$, the quantum mutual information of fermions at the nonequilibrium steady states are both increased in the localized and delocalized phases just because of the subsystem A has one more bond spin. In the localized and delocalized phases, the area law scaling of fermions and volume law scaling of spins are still present obviously. The non-Hermitian quantum disentangled liquids are independent of the partitioning method of whole system.

Supplementary References

1. Essler, F. H. L. & Fagotti, M. Quench dynamics and relaxation in isolated integrable quantum spin chains. *J. Stat. Mech.-Theory E.* **2016**, 064002 (2016). URL https://doi.org/10.1088/1742-5468/2016/06/064002.
2. Smith, A. *Disorder-Free Localization* (Springer International Publishing, New York, 2019). URL https://www.springer.com/gp/book/9783030208509.
3. Kramer, B. & MacKinnon, A. Localization: theory and experiment. *Rep. Prog. Phys.* **56**, 1469 (1993). URL https://dx.doi.org/10.1088/0034-4885/56/12/001.
4. Kawabata, K. & Ryu, S. Nonunitary scaling theory of non-Hermitian localization. *Phys. Rev. Lett.* **126**, 166801 (2021). URL https://link.aps.org/doi/10.1103/PhysRevLett.126.166801.
5. Luo, X., Ohtsuki, T. & Shindou, R. Transfer matrix study of the anderson transition in non-hermitian systems. *Phys. Rev. B* **104**, 104203 (2021). URL https://link.aps.org/doi/10.1103/PhysRevB.104.104203.